Journal of Alloys and Compounds 509S (2011) S202–S205

Contents lists available at ScienceDirect

Journal of Alloys and Compounds

journal homepage: www.elsevier.com/locate/jallcom

Microstructure observation using MeV-electron-irradiation-induced amorphization

Takeshi Nagase[a,b,*], Akihiro Nino[c], Yukichi Umakoshi[d]

[a] Research Center for Ultra-High Voltage Electron Microscopy, Osaka University, 7-1, Mihogaoka, Ibaraki, Osaka 567-0047, Japan
[b] Division of Materials and Manufacturing Science, Graduate School of Engineering, Osaka University, 2-1, Yamada-Oka, Suita, Osaka 565-0871, Japan
[c] Department of Materials Science and Engineering, Faculty of Engineering and Resource Science, Akita University, 1-1, Tegatagakuen-machi, Akita-City 010-8502, Japan
[d] National Institute for Materials Science, 1-2-1 Sengen, Tsukuba, Ibaraki 305-00471, Japan

ARTICLE INFO

Article history:
Received 18 June 2010
Received in revised form
17 November 2010
Accepted 8 December 2010
Available online 16 December 2010

Keywords:
Irradiation effects
Metallic glasses
Solid-state amorphization
High-voltage electron microscopy

ABSTRACT

MeV electron irradiation can stimulate solid-state amorphization in some intermetallic compounds. The irradiation induced amorphization phenomenon facilitates a clearer observation of the composite microstructure of the compounds. MeV electron irradiation is applied to a composite structure containing intermetallic compound “A,” which undergoes solid-state amorphization and crystalline phase “B,” which does not undergo amorphization. The composite structure transforms into a mixture of amorphous and crystalline phases by the irradiation. The distribution of A and B in the structure can hence be easily determined. High-voltage electron microscopy (HVEM) offers a unique microstructure observation technique that uses the difference between the sensitivities of compounds to undergo solid-state amorphization when MeV electron irradiation is applied to them.

1. Introduction

Amorphous alloys and metallic glasses are produced by thermal processes such as liquid-to-glass (L–G) transition, which can be conducted by liquid quenching (LQ) [1,2]. These alloys and glasses can also be produced by solid-state amorphization (SSA) processes such as crystal-to-glass (C–G) transition, which can be conducted by mechanical processes at temperatures below the glass transition temperature (T_g). Among the numerous mechanical processes for understanding the SSA mechanism, such as ion and neutron irradiation and severe plastic deformation, the observation of electron-irradiation-induced amorphization [3–5] by high-voltage electron microscopy (HVEM) is an important technique. HVEM is used for the simultaneous achievement of the stimulation of SSA and the in situ observation of the SSA process. Systematic theoretical and experimental studies have been conducted on electron-irradiation-induced SSA to understand the SSA mechanism [6,7]; it was clarified that the tendency of metallic materials to undergo SSA under electron irradiation is related to the position of these compounds in the temperature–composition (T–C) phase diagram [6]. The closer the intermetallic compound is positioned to the liquidus valley in the T–C diagram, the stronger is its tendency to undergo SSA. Okamoto et al. have proposed the generalized Lindemann melting (GLM) criterion and have theoretically suggested that amorphization is a kinetically constrained melting process [7].

Electron-irradiation-induced SSA by HVEM is useful for the above-described research on the SSA mechanism and also for the evaluation of crystalline material microstructure [8]. In this paper, we report on the concept and demonstration of microstructure observation by using MeV-electron-irradiation-induced amorphization.

2. Concept of microstructure observation by using MeV-electron-irradiation-induced amorphization

A clear understanding of the difference between the amorphization tendencies of different crystalline phases provides a unique opportunity for identifying the mixture of the crystalline phases. Fig. 1 shows a schematic illustration of the microstructure evaluation by MeV-electron-irradiation-induced amorphization. Fig. 1(a) shows a composite structure containing intermetallic compound “A,” which undergoes solid-state amorphization, and a crystalline phase “B”, which does not undergo amorphization; phase B includes solid solutions and/or intermetallic compounds with a high phase stability against amorphization. In general, the identification of A and B in a conventional polycrystalline com-

* Corresponding author at: Research Center for Ultra-High Voltage Electron Microscopy, Osaka University, 7-1, Mihogaoka, Ibaraki, Osaka 567-0047, Japan. Tel.: +81 668797941; fax: +81 668797942.
E-mail address: t-nagase@uhvem.osaka-u.ac.jp (T. Nagase).

0925-8388/$ – see front matter
doi:10.1016/j.jallcom.2010.12.051

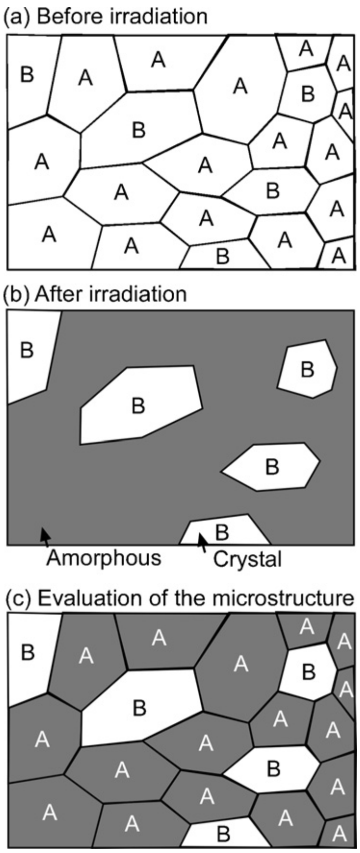

Fig. 1. Schematic illustration of microstructure obtained by MeV-electron-irradiation-induced amorphization. The composite structure contains intermetallic compound "A," which undergoes solid-state amorphization and crystalline phase "B" which does not undergo amorphization. (a) TEM microstructure before MeV electron irradiation, (b) TEM microstructure after MeV electron irradiation, and (c) composite microstructure of "A" and "B." Each crystalline phase can be identified by the occurrence of MeV-electron-irradiation-induced amorphization.

posite is difficult if there is no significant difference between A and B with regard to size and morphology. After the MeV electron irradiation is applied to the structure, only A converts to an amorphous phase, whereas B maintains the crystalline structure. The microstructure shown in Fig. 1(b) indicates an amorphous matrix in which crystalline phases B are embedded. Fig. 1(c) shows the composite microstructure of A and B; the crystalline phases can be identified by comparing the microstructures before and after irradiation (Figs. 1(a) and (b), respectively). HVEM is a unique microstructure observation technique that uses the difference between the sensitivities of compounds to undergo solid-state amorphization when MeV electron irradiation is applied to them.

3. Experimental procedure

In the present study, the microstructure of a rapidly solidified $Fe_{89.5}Nd_{10.5}$ alloy was evaluated through MeV-electron-irradiation-induced amorphization. A master ingot of $Fe_{89.5}Nd_{10.5}$ alloy was prepared from pure Fe and Nd (more than 99% purity) in a highly purified Ar atmosphere using a conventional arc-melt technique. A rapidly quenched ribbon was produced from the ingot by a single roller melt-spinning method at a roll surface velocity of $42\,ms^{-1}$ in Ar atmosphere. The microstructure before irradiation was determined by X-ray diffraction (XRD) pattern analysis and transmission electron microscopy (TEM). Thin foils for TEM observation and electron irradiation by HVEM were prepared from the ribbon using an ion-milling technique. The foils were electron irradiated in Osaka University using the ultra-high voltage electron microscope (UHVEM; H-3000) operated at an acceleration voltage of 2.0 MV. This acceleration voltage is believed to be higher than the threshold acceleration voltage required for initiating an electron knock-on effect in Fe and Nd. Electron irradiation was carried out at 104 K. The temperature was maintained within ±5 K of the desired value during electron irradiation. The applied dose rate was selected as $7.0 \times 10^{24}\,m^{-2}\,s^{-1}$. Changes in the bright-field (BF) images and selected area diffraction (SAD) patterns during electron irradiation were observed in situ using a UHVEM at 2.0 MV. The effect of additional electron irradiation during in situ TEM observations was negligible because of the low dose rate.

Table 1
Intermetallic compounds reported to have undergone solid-state amorphization when MeV electron irradiation is applied to them. Most of the data were obtained by a research group at Osaka University using an ultra-high voltage electron microscope (HU-2000 and H-3000); electron irradiation was performed at an acceleration voltage of 2 MV. The temperature during the evaluations was kept at 298 K and below; the dose rate evaluated using a Faraday cup was of the order of $1 \times 10^{24}\,m^{-2}s^{-1}$ [6,10,11].

Occurrence of solid-state amorphization under MeV electron irradiation	
Yes Group "A"	No Group "B"
Al_9Co_2	Al_2Au
Al_7Cr	Al_5Co_2
Al_5Cr	Al_9Cr_4
Al_4Cr	Al_8Cr_5
Al_3Fe	Al_2Cu
Al_6Mn	$AlCu(\eta_2)$
Al_4Mn	Al_5Fe_2
$Al_{10}V$	Al_2Fe
$Al_{45}V_7$	AlFe
$Al_{23}V_4$	Al_3Mn
Al_2Zr	$Al_{11}Mn_4$
Al_3Zr_2	$AlMn\ (\gamma_2)$
AlZr	$Al_{12}Mo$
Al_4Zr_5	Al_8Mo_3
Al_3Zr_4	Al_3Ni
Al_2Zr_3	Al_3Ni_2
$AlZr_2$	AlNi
BCo_2	$AlNi_3$
BCo_3	Al_3Ti
BFe_3	Al_3V
B_3Ni_4 (o)	Al_8V_5
BNi_2	$Al_{12}W$
Co_2Ti	Al_3Zr
Cr_2Zr	$AlZr_3$
Cu_3Ti_2	BCo
Cu_4Ti_3	BFe_2
CuTi	BNi
$CuTi_2$	B_3Ni_4 (m)
$Cu_{10}Zr_7$	BNi_3
CuZr	CoTi
$CuZr_2$	Cr_2Ti
$Fe_{17}Nd_2$	Cu_4Ti
Fe_2Ti	FeTi
$FeZr_2$	$NbNi_3$
$FeZr_3$	Ni_3Ti
Mn_2Ti	$Fe_4Nd_{1.1}B_4$
MoNi	
Nb_7Ni_6	
NiTi	
$NiTi_2$	
Ni_3Zr	
NiZr	
$NiZr_2$	
$PdZr_2$	
Pt_3Zr_5	
$Fe_{23}Nd_2B_3$	
$Fe_{14}Nd_2B$	
$Fe_{81}Zr_9B_{10}$	
ZrAlNi	

4. Results and discussion

Fig. 2 shows the typical example of the microstructure observation using MeV electron irradiation induced amorphization in a rapidly solidified melt-spun $Fe_{89.5}Nd_{10.5}$ alloy [8,9]. Fig. 2(a) shows the XRD pattern of the $Fe_{89.5}Nd_{10.5}$ alloy; the constituent phases can be identified as a mixture of α-Fe and $Fe_{17}Nd_2$ intermetallic compound. Table 1 lists the intermetallic compounds that have been reported to undergo SSA when MeV electron irradiation is applied to them [6,10,11]. Most of the data were obtained by a

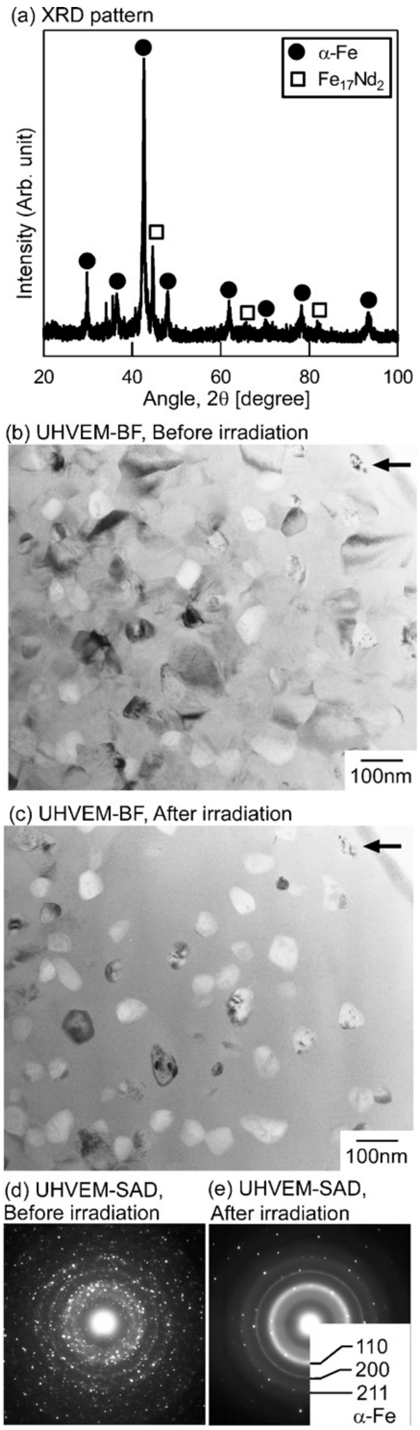

Fig. 2. The observed microstructure of a rapidly solidified melt-spun $Fe_{89.5}Nd_{10.5}$ alloy after it undergoes MeV-electron-irradiation-induced amorphization; this alloy is prepared by a single roller melt-spinning method. (a) XRD pattern of $Fe_{89.5}Nd_{10.5}$ alloy. The constituent phases are identified as a mixture of α-Fe and $Fe_{17}Nd_2$ intermetallic compound. (b) Bright-field (BF) image of specimen before irradiation. (c) BF image after electron irradiation for 600 s and a total dose of $4.2 \times 10^{26}\ m^{-2}$. (d) Corresponding selected area diffraction (SAD) pattern before the irradiation. (e) SAD pattern after the irradiation. Electron irradiation was performed using an ultra-high voltage electron microscope (UHVEM; H-3000) at 104 K. The acceleration voltage is 2.0 MV, and the dose rate is $7.0 \times 10^{24}\ m^{-2}\ s^{-1}$. Only $Fe_{17}Nd_2$undergoes solid-state amorphization, while α-Fe is stable against irradiation. The distribution of α-Fe phase and $Fe_{17}Nd_2$ can be clearly determined by the irradiation [10,11].

research group at Osaka University using a UHVEM (HU-2000 and H-3000); electron irradiation was applied at an acceleration voltage of 2.0 MV, and the temperature was maintained at 298 K or less. The dose rate, evaluated using a Faraday cup, was of the order of $1 \times 10^{24}\ m^{-2}\ s^{-1}$. Table 1 indicates that $Fe_{17}Nd_2$ belongs to group "A" which undergoes solid-state amorphization induced by MeV electron irradiation. On the other hand, the α-Fe phase belongs to group "B" as the solid-state amorphization of α-Fe solid solution was not reported. Fig. 2(b) shows the BF image of a composite structure of α-Fe and $Fe_{17}Nd_2$ intermetallic compound in melt-spun $Fe_{89.5}Nd_{10.5}$ alloy before it is irradiated. The black arrow in Fig. 2(b) and (c) is a marker. A polycrystalline structure with a crystal grain size of the order of 100 nm can be observed in the figure. The identification of each crystalline grain is impossible only in Fig. 2(b). The SAD pattern in Fig. 2(d) shows the Debye rings corresponding to α-Fe and $Fe_{17}Nd_2$. The BF image of the composite structure before irradiation (Fig. 2(b)) is in agreement with the schematic illustration shown in Fig. 1(a). The BF image and SAD pattern are drastically changed after the MeV electron irradiation. The BF image irradiated for 600 s (Fig. 2(c)) shows crystalline grains and an amorphous matrix. This BF image is in agreement with the schematic illustration shown in Fig. 1(b). The SAD pattern (Fig. 2(e)) shows Debye rings corresponding to α-Fe and newly appeared halo rings, while it does not show Debye rings corresponding to $Fe_{17}Nd_2$. In Fig. 2(c), the crystalline grains that remain after the irradiation are identified to be those of α-Fe solid solution, while the crystalline grains that convert to an amorphous phase are identified to be those of $Fe_{17}Nd_2$ intermetallic compound. The distribution of the α-Fe phase and $Fe_{17}Nd_2$ can hence be clearly evaluated after the irradiation has been performed [10,11].

The tendency of metallic materials to undergo SSA when electron irradiation is applied to them is related to the position of these materials in the temperature–composition (T–C) phase diagram [6]. The intermetallic compounds that lie close to the liquidus valley in the T–C diagram show a strong tendency to undergo SSA, while those intermetallic compounds that are far from the liquidus valley do not. The effect of the position of an intermetallic compound in the phase diagram on its glass-forming ability (GFA) during electron-irradiation-induced SSA is greater than the effects of the structure [6,12,13], transition temperature [6], and solubility [6,14,15] of the compound. In other words, intermetallic compounds whose positions coincide with a deep eutectic exhibit high GFA through irradiation-induced SSA. Fig. 3(a) shows the relationship between the occurrence of MeV electron-irradiation-induced amorphization in an intermetallic compound and the LQ induced amorphous phase formation in an alloy whose composition is the same as that of an irradiated intermetallic compound [16]; the information regarding the amorphous phase formation is obtained from previously reported experimental data. It can be observed that the intermetallic compounds whose composition is in the LQ induced amorphous phase formation range exhibit a strong tendency to undergo SSA. Fig. 3(b) shows a Fe–Nd binary phase diagram with the composition range for the LQ induced amorphous phase formation. The only Fe–Nd binary intermetallic compound that can be observed in the thermal equilibrium phase diagram is the $Fe_{17}Nd_2$. An amorphous phase formation was reported in a wide composition range in the binary Fe–Nd alloy system [16]. $Fe_{17}Nd_2$ lies in the composition range for LQ induced amorphous phase formation, indicating that $Fe_{17}Nd_2$ lies in the metastable deep eutectic in Fe and Nd solid solutions. The occurrence of irradiation induced SSA in $Fe_{17}Nd_2$ intermetallic compound can be explained by their position in the phase diagram.

As shown in Table 1, various intermetallic compounds such as metal–metal type binary Al_9Co_2, metal–metalloid type binary Co_2B, and ternary $Fe_{14}Nd_2B$ were observed to undergo SSA. Thus

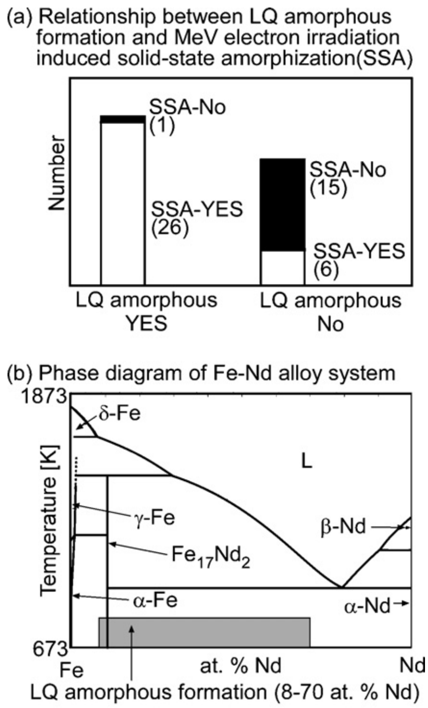

Fig. 3. Relationship between the occurrence of MeV electron-irradiation-induced amorphization in an intermetallic compound and the liquid quenching (LQ) induced amorphous phase formation in an alloys whose composition is the same as that of an irradiated intermetallic compound (a), and the Fe–Nd binary phase diagram with the composition range for the LQ induced amorphous phase formation (b).

far, 50 of 84 intermetallic compounds have been found to undergo SSA [6,10,11]; this phenomenon is commonly observed in metallic materials. This indicates that crystalline composite materials containing the intermetallic compounds belonging to the group "A" in Table 1 can be analyzed using the newly proposed technique. On the basis of the experimental database shown in Table 1, MeV electron irradiation technique by HVEM offers a unique opportunity to evaluate the microstructure of crystalline composites.

5. Conclusions

In the present study, we proposed the HVEM technique for the microstructure evaluation of polycrystalline materials and particularly for the identification of each crystalline grain. HVEM is a unique microstructure observation technique that uses the difference between the sensitivities of compounds to undergo solid-state amorphization when MeV electron irradiation is applied to them.

Acknowledgements

This study was supported by Priority Assistance for the Formation of Worldwide Renowned Centers of Research-The Global COE Program (Project: Center of Excellence for Advanced Structural and Functional Materials Design) from the Ministry of Education, Culture, Sports, Science and Technology (MEXT), Japan. The authors would like to thank Prof. H. Mori for helping us with useful discussions.

References

[1] T. Masumoto, Materials Science of Amorphous Metals, Ohm Publication, Tokyo, 1982 (in Japanese).
[2] A. Inoue, Acta Mater. 48 (2000) 279–306.
[3] G. Thomas, H. Mori, H. Fujita, R. Sinclair, Scripta Mater. 16 (1982) 589–592.
[4] H. Mori, H. Fujita, Jpn. J. Appl. Phys. 21 (1982) L494–L496.
[5] A. Mogro-Camprero, E.L. Hall, J.L. Walter, A.J. Ratkowski, in: S.T. Picraux, W.J. Choyke (Eds.), Metastable Materials Formation by Ion Implantation, North-Holland, Amsterdam, 1982, pp. 203–208.
[6] H. Mori, in: Y. Sakurai, Y. Hamakawa, T. Masumoto, K. Shirae, K. Suzuki (Eds.), Current Topics in Amorphous Materials: Physics and Technology, Elsevier Science Publishers, Amsterdam, 1997, pp. 120–126.
[7] P.R. Okamoto, N.Q. Lam, L.E. Rehn, Physics of crystal-to-glass transformations, in: H. Ehrenreich, F. Spaepen (Eds.), Solid State Physics, vol. 52, Academic Press, San Diego, 1999.
[8] T. Nagase, A. Nino, Y. Umakoshi, Materia Jpn. 48 (2009) 607 (in Japanese).
[9] A. Nino, T. Nagase, Y. Umakoshi, Mater. Trans. 48 (2007) 1659–1664.
[10] T. Nagase, Mater. Jpn. 47 (2008) 519–523.
[11] T. Nagase, K. Takizawa, A. Nino, Y. Umakoshi, Proc. of Mater. Res. Soc. 2008 Fall Meeting, 1148, Boston, 2009, U05-49-08 1-6.
[12] H. Matzka, J.L. Whitton, Can. J. Phys. 44 (1966) 995–1010.
[13] T. Sakata, Doctoral thesis, Osaka University, 1994.
[14] J.L. Brimhall, H.E. Kissinger, L.A. Charlot, Radiat. Eff. 77 (1983) 273–293.
[15] D.B. Luzzi, M. Meshii, Scripta Metall. 20 (1986) 943–948.
[16] U. Mizutani, Y. Hoshino, H. Yamada, Preparation of Amorphous Alloys, Agne, Tokyo, 1986 (in Japanese).